

# Influence of Phenazine Structure on Polaron Formation in Polyaniline: In Situ Electron Spin Resonance—Ultraviolet/Visible—Near-Infrared Spectroelectrochemical Study

Evgenia Dmitrieva,<sup>†</sup> Yutaka Harima,<sup>‡</sup> and Lothar Dunsch<sup>\*,†</sup>

Department of Electrochemistry and Conducting Polymers, Leibniz Institute of Solid State and Materials Research, Helmholtzstrasse 20, D-01171 Dresden, Germany, and Graduate School of Engineering, Hiroshima University, 1-4-1 Kagamiyama, Higashi-Hiroshima 739-8527, Japan

Received: July 30, 2009; Revised Manuscript Received: October 19, 2009

The role of the phenazine structure in the stabilization of charged states in polyaniline was studied by in situ electron spin resonance (ESR)—UV/vis—near-infrared (NIR) spectroelectrochemistry of polyaniline and the copolymers of aniline and a phenazine derivative (3,7-diamino-5-phenylphenazinium chloride, phenosafranin). It is shown that the copolymer can be prepared by electropolymerization, and its structure was confirmed by mass spectrometry and IR spectroscopy. The electrochemistry of polyaniline and its copolymer pointed to preferred stabilization of a polaron pair in the charged states at the initial charge transfer reaction instead of polarons that are formed by equilibrium reaction at higher electrode potentials. A second polaron pair is detected for higher doped states of the polymer films. A mechanism of the formation of charged states in polyaniline and their equilibrium is given. It is shown that in situ ESR—UV/vis—NIR spectroelectrochemistry is the method of choice to differentiate between polarons and polaron pairs in their potential-dependent formation. Thus, by this in situ spectroelectrochemical method the influence of phenazine structure on the formation of polarons in aniline polymers and copolymers can be followed.

## Introduction

Polyaniline (PANI) is one of the most-studied conducting polymers due to its applications. Reversible charge injection into conjugated, semiconducting macromolecular chains, or so-called “doping”, leads to a wide variety of interesting and important applications of PANI.<sup>1</sup> PANI is used in energy storage devices (because of higher capacitance values and more symmetrical charge/discharge cycles due to high surface area);<sup>2</sup> in electrochromic devices (because of a reversible optical change in a polymer induced by an external voltage);<sup>3</sup> in sensors (because of the strong and reversible influence of oxidation/reduction, protonation/deprotonation, and conformational changes on electrical and optical properties of polymer);<sup>4</sup> and in molecular electronics devices like diodes, light-emitting diodes, and field effect transistors (as a p-type semiconductor).<sup>5</sup>

The chemical structure of PANI is often given by a linear model with three oxidation states of polymer: completely reduced leucoemeraldine, intermediate emeraldine, and fully oxidized pernigraniline bases (Figure 1). On the basis of these structures, the well-accepted *polaron–bipolaron model* for conducting polymers is interpreted as follows: the completely reduced polymer segments, which are diamagnetic; the singly oxidized form of a polymer segment (polaron) with spin  $s = 1/2$ ; and the doubly oxidized form (bipolaron), which is diamagnetic.<sup>6</sup> According to the Fesser–Bishop–Campbell model, the polymer in the reduced state has one  $\pi$ – $\pi^*$  transition, the polaronic state has two optical transitions, and in bipolaronic state only one optical transition is observed.<sup>7</sup> The scheme of the energy levels of neutral polymer, positive polaron, and bipolaron as discussed in the literature is presented in Figure

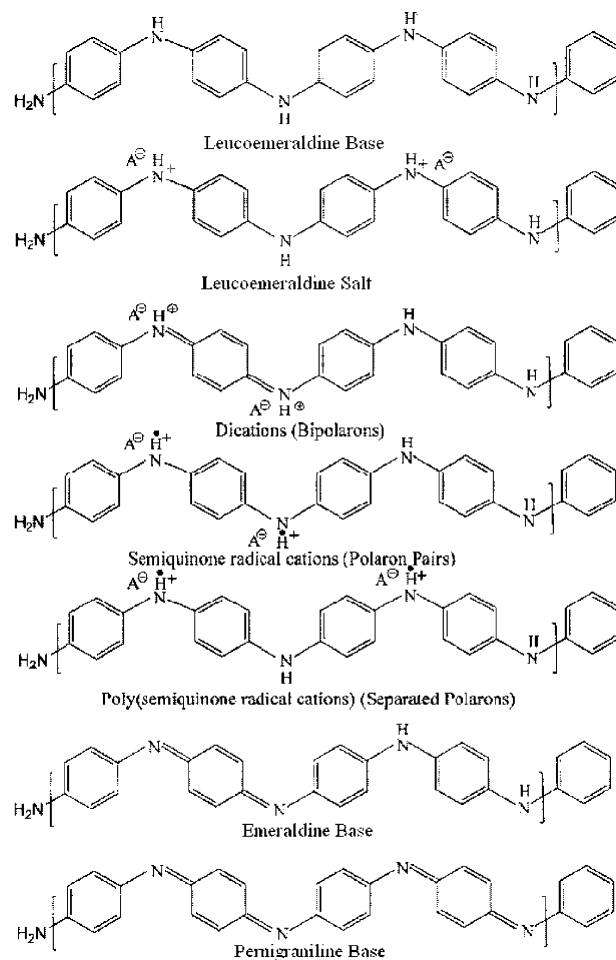


**Figure 1.** Linear chemical structures of PANI and their different oxidation states.

\* Corresponding author: phone: +49-351-4659-660; fax: +49-351-4659-811; e-mail: L.Dunsch@ifw-dresden.de.

<sup>†</sup> Leibniz Institute of Solid State and Materials Research.

<sup>‡</sup> Hiroshima University.

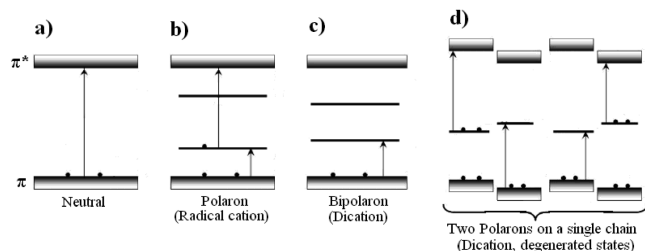


**Figure 2.** Scheme of the energy levels of neutral polymer, positive polaron, bipolaron, and polaron pair.<sup>10</sup>

2a–c. The absorption peaks in the UV/vis–near-infrared (NIR) spectra of PANI in aprotic solvents observed at 440 and 780 nm are characteristic for the separate polarons and can be assigned as the transitions from polaron band to  $\pi^*$ -band and  $\pi$ -band to polaron band, respectively.<sup>8</sup> The peak at 440 nm and a steadily increasing “free-carrier tail” starting from  $\sim 1000$  nm to the infrared region are due to delocalized polarons that are observed in protic solvents.<sup>8,9</sup> The “free-carrier tail” in the IR region is characteristic of metallic conductive materials. Brédas and co-workers<sup>10</sup> studied the redox states of oligothiophenes with different lengths to follow polarons and bipolarons in short-chain oligomers. As the electronic structure of large oligomers differs from the expected features of a bipolaron, they proposed “two polarons on a single chain” as a model characterized by two excitations and two absorption peaks in the UV/vis–NIR spectrum, respectively (Figure 2d). MacDiarmid et al.<sup>11</sup> showed that the protonation of the emeraldine base leads at first to the formation of a bipolaron, which transforms into a semiquinone radical cation (polaron pair) by internal redox reaction. The polaron pair dissociates later into two separated polarons [poly(semiquinone radical cation)] by Coulombic repulsion. Brazovskii et al.<sup>12</sup> studied the stability of a bipolaron in a nondegenerate conjugated polymer relative to a pair of polarons as a function of on-site Coulomb interaction and the strength of electron–phonon interaction and found a critical value of Coulomb interaction strength above which the bipolaron dissociates into a pair of polarons. More recently the equilibrium and kinetics of systems with either polarons and bipolarons or polarons and polaron pairs as charged states were compared.<sup>13</sup> The  $\pi$ -dimer (two polarons on two adjacent chains) and “two polarons on a single chain” are denoted as a polaron pair, which is not active in electron spin resonance (ESR). For the system with polaron/bipolaron, the bipolaron concentration saturates at high potentials, and the polaron concentration shows a maximum at the potential for the two-electron reaction and decreases at higher potentials. In contrast, in the system with polaron/polaron pair, both the polaron pair and polaron concentrations saturate at high potentials. Therefore, the polaron pair model is reasonable if a second oxidation step is possible

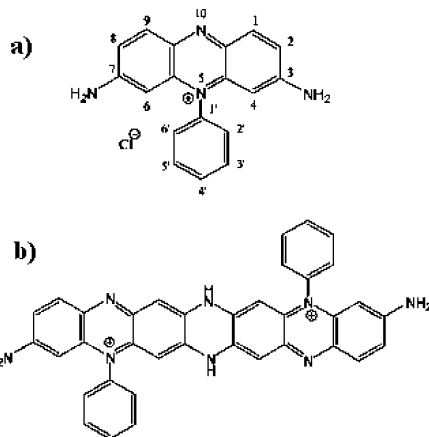


**Figure 4.** Structures of (a) phenosafranine and (b) N–C2 coupled phenosafranine dimer.<sup>30</sup>

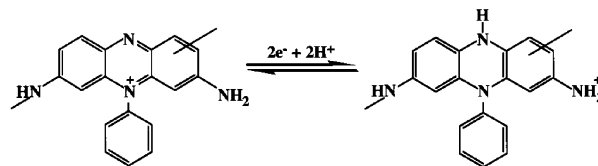


**Figure 5.** Redox reaction of polyphenosafranine.<sup>29</sup>

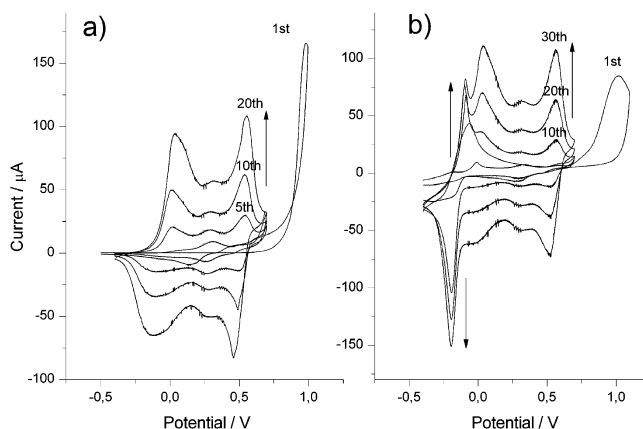


**Figure 6.** Growth of a polymer film during the potential cycling of aqueous solution of 50 mM aniline containing 0.1 M sulfuric acid and 0.01 M sodium *p*-toluenesulfonate on a laminated ITO electrode in the (a) absence and (b) presence of 5 mM phenosafranine. Scan rate: 25 mV/s.

at a standard potential near that of the first oxidation step. At lower potentials, the probability of both models is virtually the same. Miller and co-workers<sup>14</sup> suggested a *polaron– $\pi$ -dimer model* in addition to bipolarons in oxidized polythiophene. The  $\pi$ -dimer is considered as a face-to-face complex of two radical cations interacting through their  $\pi$ -orbitals. Because of the

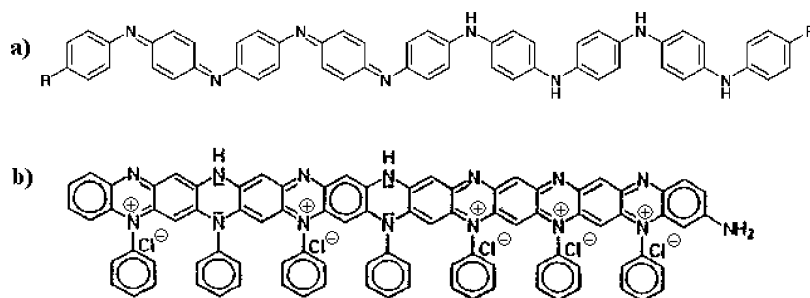


**Figure 3.** Structure of (a) linear and (b) phenazine-like<sup>26</sup> PANI.

TABLE 1: Proposed Structures of Molecule Ions Corresponding to  $m/z$  Values in the Mass Spectra

Fragment	Structure	Corresponding value of $m/z$ , a.u.
1		184
2		195
3		210
4		287
5		142
6		482
7		242
8		492
9		584

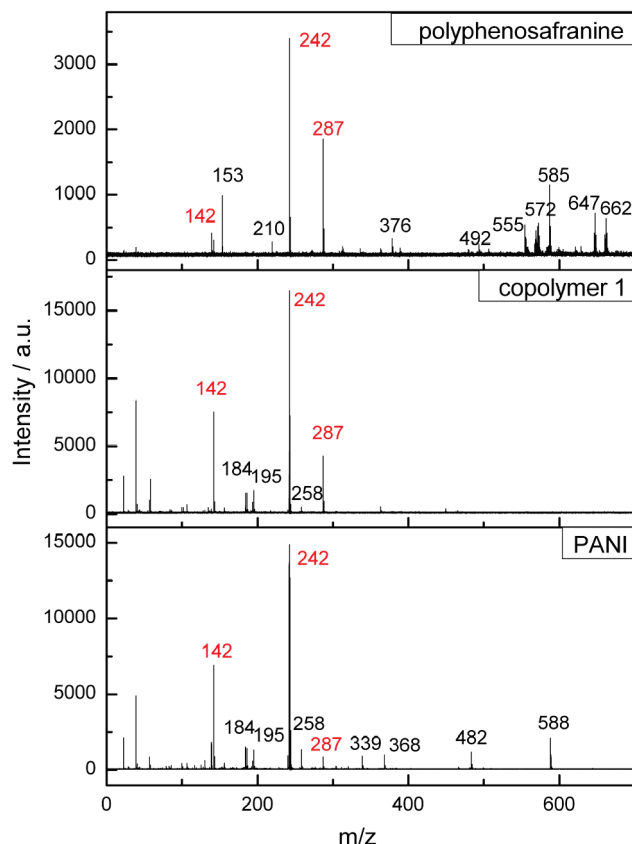


**Figure 7.** Mass spectra of electropolymerized PANI, copolymer 1, and electrochemically prepared polyphenosafranine. The mass spectra are shown in the range from  $m/z$  0 to 700.

reversible radical cation formation without further chemical reactions, the authors assumed that the cation radical forms a  $\pi$ -dimer which is quickly formed and quickly falls to pieces. We have shown recently that the most important intermediate formed during aniline polymerization, *p*-aminodiphenylamine, is a  $\pi$ -dimer of two radical cations under oxidation in acidified organic solvents.<sup>15</sup> In contrast, a *polaron*– $\sigma$ -dimer model for diphenylpolyene and oligomers of thiophene was suggested.<sup>16</sup> A fast reversible  $\sigma$ -dimerization of radicals with formation of diamagnetic dication is assumed after polaron formation, but there is no experimental proof for a polymer. The electrochemical charging/discharging mechanism of PANI was studied in detail by in situ ESR–UV/vis spectroelectrochemistry,<sup>17</sup> and it was demonstrated that the polarons (B) can also be formed by a comproportionation reaction between bipolaron (C) and neutral polymer segments (A). This redox concept is supported by the mechanism of polymer growth.<sup>18</sup> The equilibrium constant for the comproportionation reaction was determined (eq 2); it corresponds to a negative difference of the standard potentials of the first and second electron transfer and shows that the second electron transfer is energetically favored (eq 1).



Up to now, the first redox peak in the cyclovoltammogram of PANI has been attributed to the transformation of leuco-

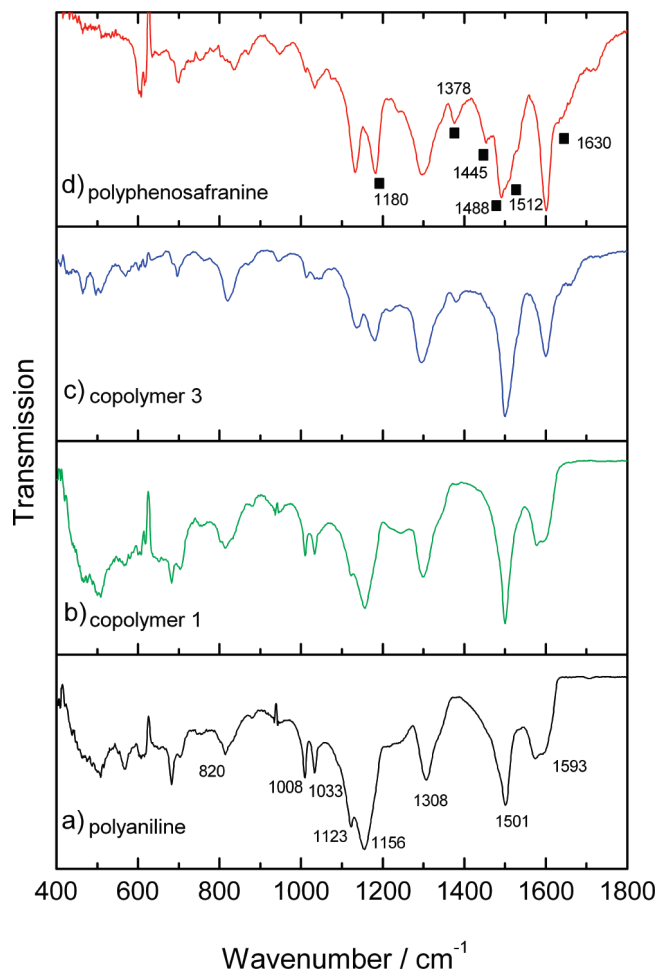


**Figure 8.** Infrared spectra of (a) electrochemically prepared PANI, (b) copolymer 1, (c) copolymer 3, and (d) polyphenosafranine (all in reduced state). The spectra are shown in the region from 400 to 1800  $\text{cm}^{-1}$ .

meraldine into emeraldine form, and the second peak to the further oxidation of emeraldine to fully oxidized pernigraniline form.<sup>19</sup> Genies et al.<sup>20</sup> studied the origin of the middle peak in the cyclovoltammogram of PANI in hydrofluoric acid solution during copolymerization of the aniline and phenazine. In this work, the middle peak of PANI was attributed to the presence of a polymer containing phenazine rings, because the intensity of the peak increases upon copolymerization of aniline with phenazine and by oxidation of aniline at a higher potential than the second voltammetric peak. Stilwell and Park<sup>21</sup> studied the growth properties of PANI. These authors assume that the middle peak in the cyclovoltammogram during aniline polymerization corresponds to the benzoquinone/hydroquinone couple produced via hydrolysis reaction, but direct proof is not given.

Harima et al.<sup>22</sup> studied mobilities of charge carriers in poly(3-hexylthiophene) as-grown film and a cast film. A clear difference was observed in the mobility versus doping level plot and the potential dependence of conductivity between the two sorts of polymer films, demonstrating that the difference is caused by a distinction in film structure. By the application of in situ reflection technique, it has been shown that the polaron lattice formation is responsible for the enhancement in mobility and stretching of polymer chains, the latter leading to the increase in the reflected light intensity.<sup>23</sup>

It is well-accepted in the scientific community of conducting polymers that PANI consists of a linear arrangement of monomers (Figure 3a). Since the early work of Willstätter and

**TABLE 2: Main Infrared Bands of Polyaniline and Their Assignments<sup>a</sup>**

wavenumber/cm <sup>-1</sup>	assignment	ref
682–704/755 w	C–H out-of-plane deformation vibration on monosubst aromatic ring	37
816 m	C–H out-of-plane deformation vibration on 1,4-subst ring	37
1033 m, 1008 m	C–H in plane deformation vibration on 1,4-subst ring	37
1156 s, 1123 s	C–H in plane deformation vibration	38
1308 s, 1340 sh	C–N stretching in primary and secondary aromatic amines	37
1378 w	C–N stretching in the neighborhood of a quinonoid ring	39
1501 s	C–C stretching (benzene ring)	40
1575 s	NH <sub>2</sub> scissoring in primary aromatic amines	37
1593 s, 1575 s	C–C stretching (quinoid ring)	40
3020–3060 m	aromatic = C–H stretching (in spectra is not shown)	37
3400–3100 m	N–H stretching in aromatic amines (in spectra is not shown)	37

<sup>a</sup> Abbreviations: sh, shoulder; s, strong; w, weak; m, medium.

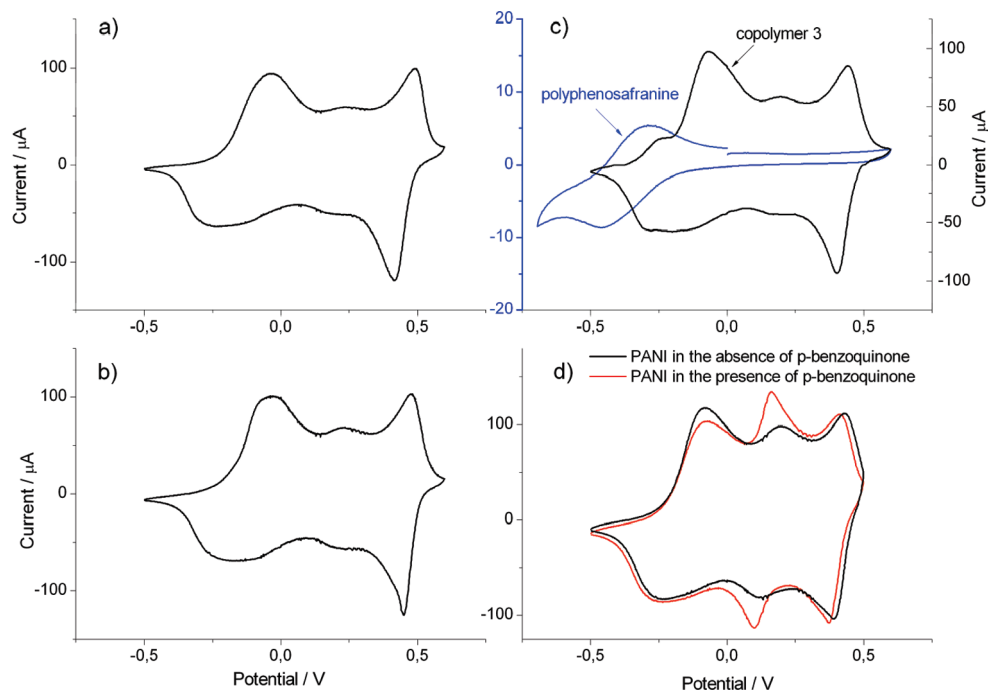


**Figure 9.** Cyclic voltammograms of (a) PANI, (b) copolymer 2, and (c) electrochemically prepared polyphenosafranine in aqueous solution of 0.1 M sulfuric acid and 0.01 M sodium *p*-toluenesulfonate on a laminated ITO electrode at a scan rate of 25 mV/s. (d) Cyclic voltammogram of PANI in supporting electrolyte with and without  $5 \times 10^{-4}$  M *p*-benzoquinone. The polymer films were electrochemically deposited by potential cycling.

Moore,<sup>24</sup> of Green and Woodhead<sup>25</sup> for chemically synthesized PANI, and of our group<sup>26</sup> for electrochemically prepared PANI, it is obvious that phenazine rings have to be considered as a part of the polymer chains (Figure 3b). The presence of substituted phenazine structural units, formed by the oxidative intramolecular cyclization of branched PANI chains, has been proved by the appearance of characteristic Fourier transform infrared (FTIR) bands at 1623, 1414, 1208, 1144, 1136, and 1108 cm<sup>-1</sup> and Raman bands at 1645–1630, 1420–1400, 1380–1365, ~575, and ~415 cm<sup>-1</sup>.<sup>27</sup> Do Nascimento et al.<sup>28</sup> demonstrated that the heating of PANI nanofibers promotes the formation of cross-linking, phenazine- and/or oxazine-like structures, of polymer, which have Raman bands at ca. 1637 (1640), 1380 (1360), and 614 (592) cm<sup>-1</sup>. In this work the spectra of heated PANI were compared with those of Safranine O (phenazine-like ring) and Nile Blue (oxazine-like ring) dyes.

While most studies on the electronic structure of PANI and the change upon doping use the linear structure model, the influence of phenazine structures on the formation of charged states in PANI has not yet been studied in detail. In this work the ESR–UV/vis–NIR spectroelectrochemistry of the copolymer of aniline and a phenazine derivative (3,7-diamino-5-phenylphenazinium chloride, phenosafranine) upon charging are

presented. The structure of phenosafranine (Figure 4a) is close to the phenazine-like structure of PANI (Figure 3b). The redox properties of electrochemically prepared polyphenosafranine were investigated at its different oxidation and protonation levels by cyclic voltammetry and electrochemical impedance spectroscopy by Komura et al.<sup>29</sup> These authors showed that phenosafranine forms an electroactive polymer upon anodic oxidation in acidic aqueous solutions. A two-electron, two-proton reduction of polyphenosafranine results in the formation of 10-hydro-5-phenylphenazine form (Figure 5). Ćirić-Marjanović et al.<sup>30</sup> oxidized phenosafranine chemically in acidic aqueous solutions. In this work it was found that the main phenosafranine dimers are formed by N–C2 and N–C4 coupling modes. Two-electron oxidation of the phenosafranine N–C2 dimer, followed by intramolecular cyclization, lead to the dimer with a ladderlike structure containing a newly formed phenazine segment (Figure 4b).

By use of in situ ESR–UV/vis–NIR spectroelectrochemistry, the role of phenazine structures in stabilization of the injected charge in PANI is studied in detail and the voltammetric behavior of PANI is explained.



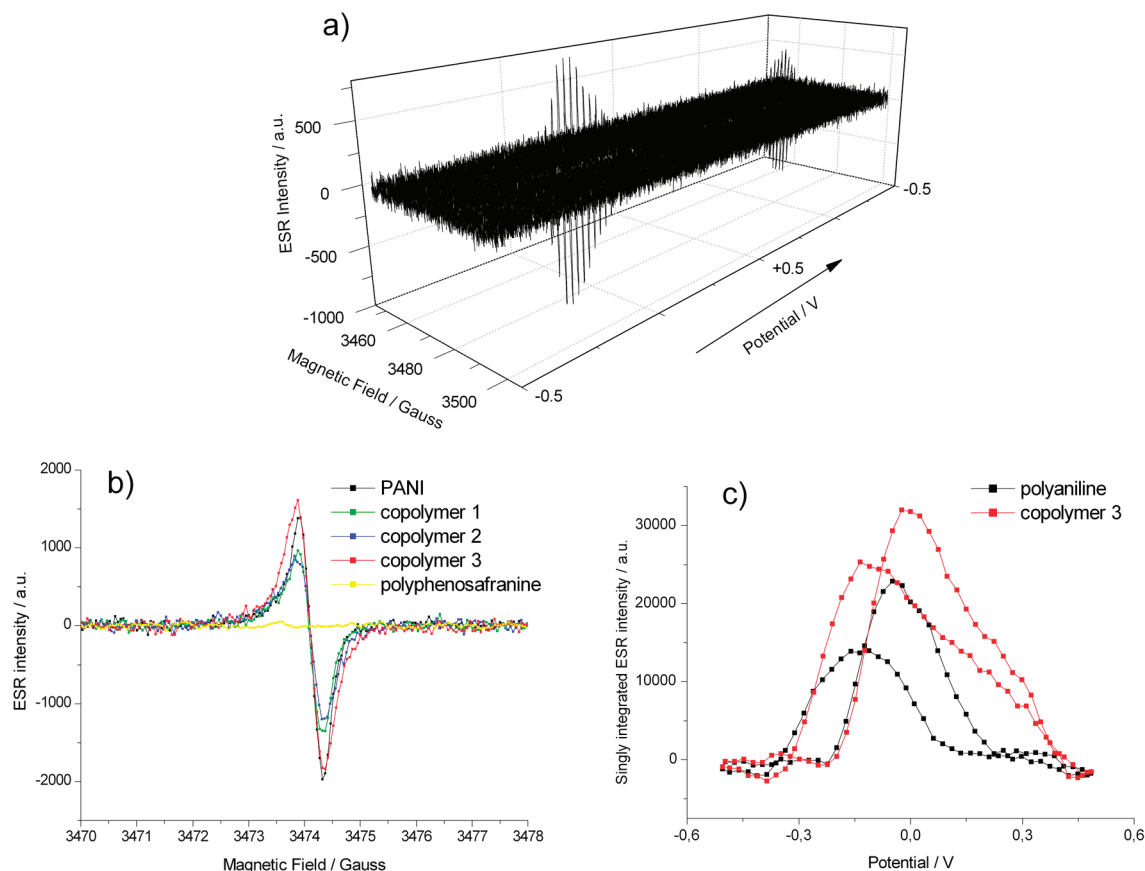


**Figure 10.** (a) Potential dependence of the ESR signal of copolymer 2 during the voltammetric scan in aqueous solution of 0.1 M sulfuric acid and 0.01 M sodium *p*-toluenesulfonate. (b) ESR signal of PANI, the different copolymers, and polyphenosafranine in the doped state. (c) Potential dependence of integrated ESR intensity of PANI and copolymer 3.

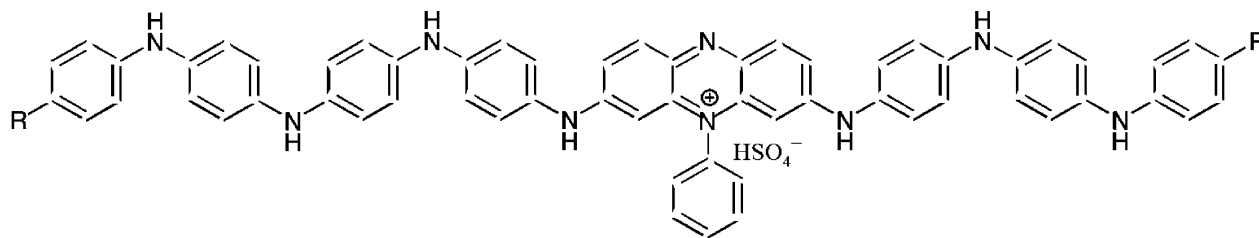


**Figure 11.** Proposed scheme of PANI and its copolymer.

## Experimental Methods

The ESR–UV/vis–NIR spectroelectrochemical technique was described earlier.<sup>17</sup> For ESR measurements, an EMX (Bruker) X-band spectrometer with 100 kHz modulation and microwave power of 2 mW was used. ESR spectra were recorded at a modulation amplitude of 0.5 G and a sweep time of 5.24 s. The standard optical cavity ER 4104 OR (Bruker) allowed the connection of two optical light guides to measure the electronic absorption spectra in situ simultaneously with the ESR spectra. For UV/vis–NIR spectroscopy, a photodiode array spectrometer (TIDAS, J&M, Analytische Mess- und Regeltechnik, Aalen, Germany) applying the Scan2017 software (J&M Analytische Mess- und Regeltechnik GmbH, Aalen, Germany) was used. In situ ESR–UV/vis–NIR spectroelectrochemical measurements were controlled by a PG 285 potentiostat (HEKA Electronic, Lambrecht, Germany) equipped with Potpulse software v. 8.53 triggering an ESR spectrometer and UV/vis–NIR diode array spectrometer. During one redox cycle, by sweeping the potential from  $-0.5$  up to  $+0.5$  V (at a scan rate of 2.5 mV/s), 80 UV/vis–NIR and 80 ESR spectra were

recorded. The spectroelectrochemical flat cell was equipped with a working electrode as a laminated indium tin oxide (ITO) electrode (thickness of 0.3 mm, specific surface conductivity of 20  $\Omega$ /square, Merck) with an area of 0.096 cm<sup>2</sup>. A rectangular black mask with a hole smaller than the active electrode surface of the laminated ITO electrode was fixed on the flat cell. The counterelectrode consists of a platinum wire. A silver chloride-coated silver wire with a thin flexible Teflon tube served as the pseudoreference electrode (all potentials here are given versus silver pseudoreference electrode). UV/vis–NIR spectra were recorded in reference and run mode. The nonelectrically contacted ITO sheet was used for the simple measurement of reference spectra, as illustrated in ref 31. By changing the position of the electrode up and down in the ESR flat cell, the reference or probe spectra were measured without any changes in the spectrometer setup. Spectroelectrochemical measurements were carried out under nitrogen atmosphere and at room temperature.

Electropolymerization was carried out in a preparative electrochemical cell in aqueous solution of 50 mM aniline,

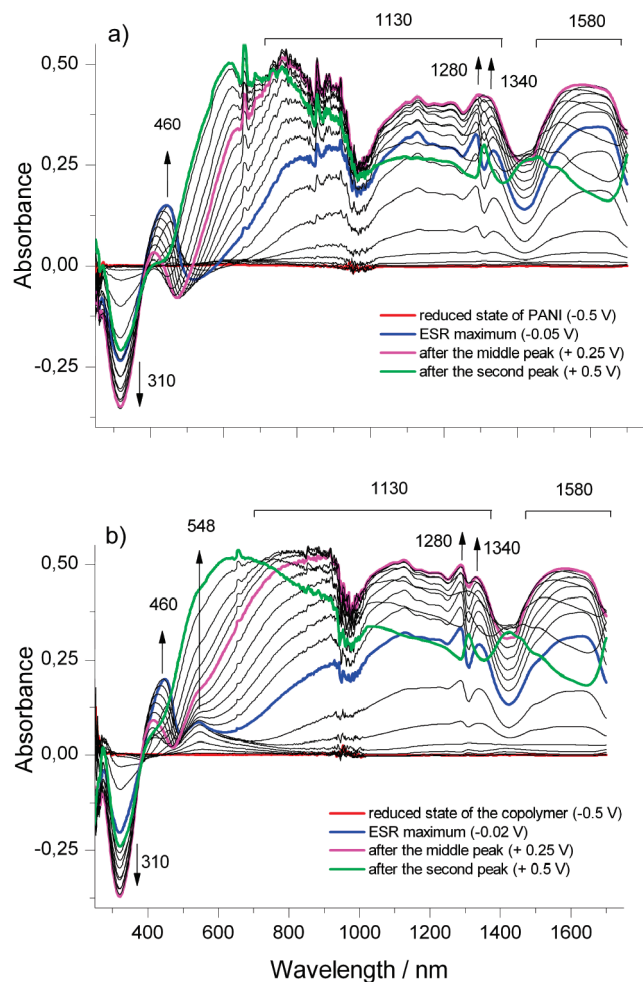


**Figure 12.** UV/vis–NIR spectra of PANI recorded in aqueous solution of 0.1 M sulfuric acid and 0.01 M sodium *p*-toluenesulfonate during the forward scan in the potential region from  $-0.5$  to  $+0.5$  V (scan rate 2.5 mV/s). The dip at ca. 1000 nm is caused by the low intensity of the light source in this range.

0.1 M sulfuric acid (Merck, 95–97%), and 0.01 M sodium *p*-toluenesulfonate (Merck, 98%). Polymer films were electrochemically deposited on an ITO electrode by potential cycling between  $-0.5$  and  $+0.5$  V at a scan rate of 25 mV/s. For initialization of the polymerization, the first scan between 0 and 1000 mV was used. For copolymerization, the same solution was used with 1, 5, and 20 mM 3,7-diamino-5-phenylphenazinium chloride (phenosafranine) (Fluka, for microscopy), denoted as copolymer 1, 2, and 3, respectively. Polyphenosafranine films were electrochemically prepared from a 5 mM phenosafranine solution in supporting electrolyte by potential cycling between  $-0.5$  and  $+1.2$  V. The chemical preparation of polyphenosafranine was carried out according to the procedure of Ćirić-Marjanović et al.<sup>30</sup> For analysis of the voltammetric behavior of PANI and the copolymer,  $5 \times 10^{-4}$  M *p*-benzoquinone (Merck, 98%) in supporting electrolyte was used.

The mass spectrometric analysis was performed with a matrix-assisted laser desorption ionization time-of-flight (MALDI-TOF) spectrometer, Biflex III (Bruker Daltonik GmbH, Germany), in laser desorption ionization (LDI) mode within a mass range from  $m/z$  0 to 1900. FTIR spectra of PANI and the copolymers were measured on a silicon crystal at room temperature in transmission mode by an IFS 66v spectrometer (Bruker, Germany) at a resolution of 2  $\text{cm}^{-1}$ . For mass spectrometry and FTIR measurements, the polymer films were prepared on platinum electrodes

by potential cycling, dissolved in the reduced state in dimethyl sulfoxide (DMSO) and evaporated at 80  $^{\circ}\text{C}$ .

## Results and Discussion

Figure 6 presents the growth of a polymer film during the electropolymerization of aniline without and with phenosafranine by potential cycling in the electrolyte solution. The cyclic voltammogram of PANI in the presence of phenosafranine has an additional reversible voltammetric peak at ca.  $-0.1$  V (Figure 6b). The peak was attributed to oxidation of 3,7-diamino-10-hydro-5-phenylphenazine to 3,7-diamino-5-phenylphenazine.<sup>29</sup> This peak increases with an increasing number of cycles. It points to the copolymerization of aniline and phenosafranine by electrochemical synthesis.

The presence of the phenazine structure in PANI and of the aniline–phenosafranine copolymer has been confirmed by mass spectrometry (Figure 7). The mass peak at  $m/z = 287$ , which is observed in the mass spectra of all polymer structures, corresponds to the phenazine-like<sup>32</sup> or linear structures of PANI (Table 1, structure 4). We suppose that the peak at  $m/z = 142$  in PANI and its copolymer can be attributed to doubly charged phenosafranine molecule (Table 1, structure 2). The peaks at  $m/z = 242$  correspond to doubly charged fragment ions that have phenazine-like rings (Table 1, structure 7). It has been proved by mass spectrometry that both PANI and the aniline–phenosafranine copolymer have phenazine-like units in their structure. Therefore, the role of phenazine structures in PANI should be taken into account in all studies of the charge transfer reaction of this conducting polymer.

Further studies of the polymer and the copolymer composition have been done by IR spectroscopy. The infrared spectra of PANI and the aniline phenazine copolymer, respectively, were analyzed with respect to the phenazine structure (Figure 8). Assignment of the vibrations in the IR spectra is given in Table 2. The IR spectra of PANI and the aniline–phenosafranine copolymers are very similar. For reference, the spectrum of electrochemically prepared polyphenosafranine was analyzed, giving additional bands at 1630, 1530, 1512, 1488, 1445, 1378, and 1180  $\text{cm}^{-1}$  (Figure 8d). The peaks at 1630 and at 1488 and 1378  $\text{cm}^{-1}$  in polyphenosafranine can be attributed to C–C and C=N stretching modes in a phenazine-like ring structure.<sup>33,34</sup> These bands are also present in the IR spectra of copolymer 3. The band at 1530  $\text{cm}^{-1}$  is present in the IR spectrum of phenosafranine and can be associated with a C–C and C=N stretching mode in a phenosafranine ring. This band is also present in pyridinium salts, 1-(4-pyridyl)pyridinium chloride hydrochloride, phenazine methosulfate, and safranine O, which have a central charged nitrogen atom in their structures, but it is shifted in pyridine and phenazine to ca. 1510  $\text{cm}^{-1}$ .<sup>33,35</sup> We propose that this peak can be attributed to  $\text{C}=\text{N}^{+}$  stretching vibration in a phenosafranine unit in the PANI structure. Such a structure could be formed by aniline coupling reactions in the ortho position followed by an intramolecular cyclization reaction. The bands at 1512 and 1445  $\text{cm}^{-1}$  in polyphenosafranine point to the formation of a new aromatic system in the polymeric chains and are attributable to the ring stretching vibrations in a formed phenazine segment.<sup>36</sup> This process can be also regarded as the formation of a further pyrazine ring between two adjacent phenosafranine units (Figure 4b). These bands are present as a shoulder in the IR spectrum of copolymer 3 but absent in the starting phenosafranine and PANI spectra. The additional peak found at 1180  $\text{cm}^{-1}$ , which is present as a shoulder in the spectra of PANI and copolymer 1, corresponds to a C–H in-plane deformation vibration.<sup>37</sup> This

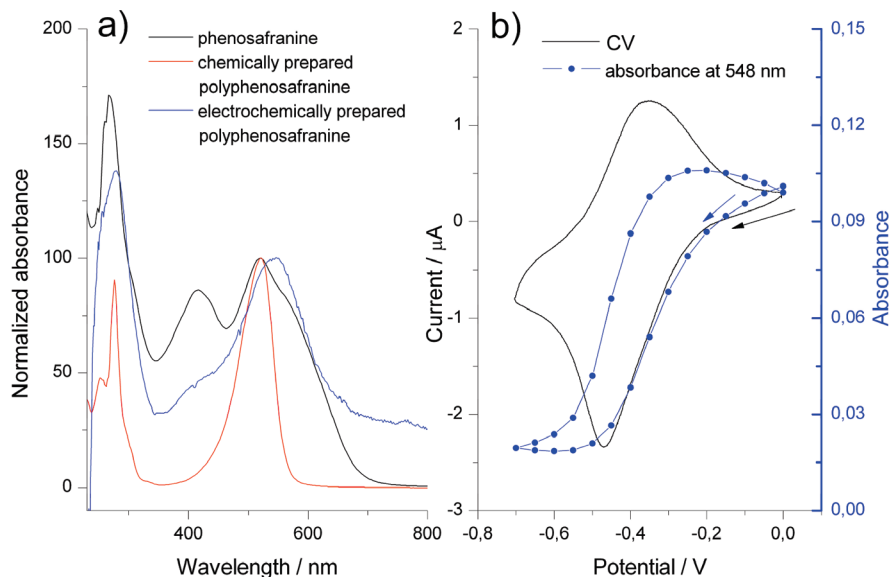


**Figure 13.** (a) Normalized UV/vis spectra of phenosafranine and of chemically and electrochemically prepared polyphenosafranine in the reduced state in aqueous solution of 0.1 M sulfuric acid and 0.01 M sodium *p*-toluenesulfonate. The spectrum of electrochemically prepared polyphenosafranine was recorded on an ITO electrode. (b) Cyclovoltammogram of the electrochemically prepared polyphenosafranine and potential dependence of the absorbance at 550 nm recording on an ITO electrode during the voltammetric scan in aqueous solution of 0.1 M sulfuric acid and 0.01 M sodium *p*-toluenesulfonate.

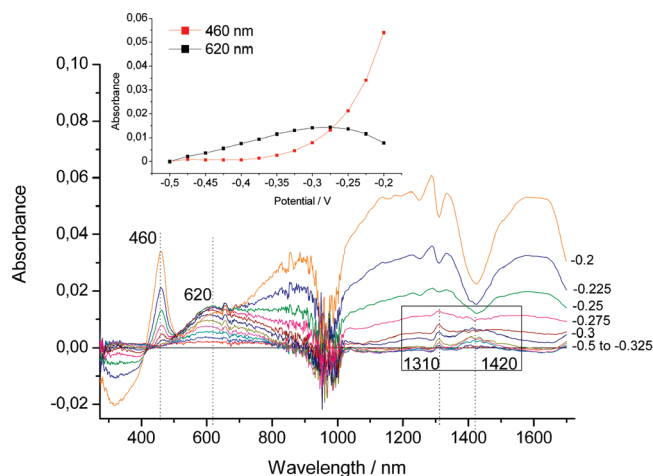


**Figure 14.** UV/vis–NIR spectra of PANI during cyclic voltammetry in the forward scan from  $-0.5$  to  $-0.2$  V at a scan rate of  $2.5$  mV/s in in aqueous solution of  $0.1$  M sulfuric acid and  $0.01$  M sodium *p*-toluenesulfonate. (Inset) Potential dependence of absorbance at  $460$  and  $620$  nm. The dip at ca.  $1000$  nm is caused by the low intensity of the light source in this range.

peak increases with increasing amounts of phenosafranine in the polymer. The band at  $835\text{ cm}^{-1}$  in polyphenosafranine can be attributed to a skeletal vibration in the phenazine ring system.<sup>33</sup> This band did not appear in the spectra of 5,10-dihydrophenazine and phenazyl hydrochloride, compounds in which conjugation of the phenazine system was disrupted.<sup>33</sup> The spectra of PANI and its copolymers have a shoulder at  $835\text{ cm}^{-1}$ .

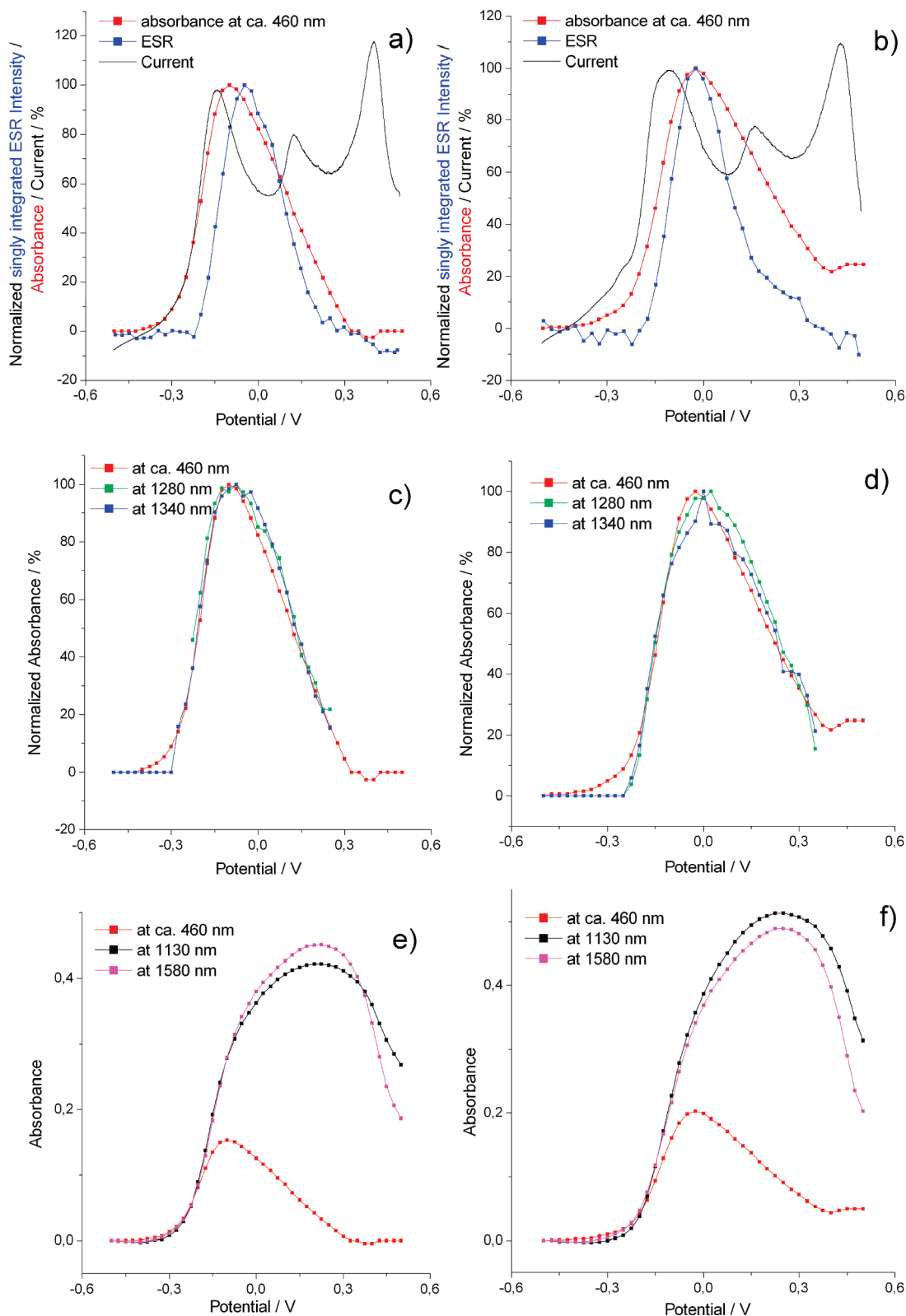
As shown by IR spectroscopy, PANI, the aniline–phenosafranine copolymers, and polyphenosafranine have similar structures consisting in all cases of phenazine ring systems.

As discussed in the literature, the presence of phenazine-like structures might be visible in the voltammetric behavior by the presence of the so-called middle peak, being of minor intensity and switching in the major redox peaks. The origin of the middle peak in cyclovoltammograms of PANI and copolymers was studied by comparison of the voltammetric behavior of different redox systems. Figure 9a,b shows cyclovoltammograms of PANI

and the copolymer that have a middle peak at ca.  $0.16$  V. These demonstrate that the insertion of phenosafranine units in PANI has no influence on the intensity of the middle peak. The cyclovoltammogram of PANI in the presence of *p*-benzoquinone gives a reversible peak at a potential of  $0.16$  V, which is close to that of the middle peak of PANI (Figure 9d). Surwade et al.<sup>41</sup> showed that the oligomers formed by mixing aniline and 1,4-benzoquinone in water without peroxydisulfate oxidant present no phenazine units in their structure. As the cyclovoltammogram of polyphenosafranine presents no peaks in this potential region (Figure 9c), the middle peak cannot be associated with the redox reaction of phenazine rings in polymer. If the middle peak corresponds to the oxidation of phenazine rings present in polymer structure according to Genies et al.,<sup>20</sup> we should see this peak in the cyclovoltammogram of polyphenosafranine, but in our experiments there are no peaks in this potential region (Figure 9c). Therefore, we suppose that the middle peak in the cyclovoltammograms of PANI is attributed to the benzoquinone/hydroquinone couple in the polymer structure, which is formed by the hydrolysis of imine groups. Copolymer 3, with the highest content of phenosafranine, has an additional peak at  $-0.23$  V during anodic scan in the cyclovoltammogram (Figure 9c), which corresponds to oxidation of phenosafranine units in the polymer chains.

The formation of charged states in PANI and the aniline–phenosafranine copolymer upon oxidation was followed by in situ ESR–UV/vis–NIR spectroelectrochemistry. As an example, the ESR response of the copolymer during the voltammetric scan is presented in Figure 10a. The ESR spectra of both PANI and the aniline–phenosafranine copolymer in the doped state are very similar and have a narrow ESR signal with line width of  $0.5$  G (Figure 10b) that is unchanged during the voltammetric scan. On the basis of the polaron–bipolaron model, the single-line ESR spectrum is attributed to the presence of polarons in polymer chains. The ESR spectrum of polyphenosafranine gives no ESR signal upon oxidation/reduction, pointing to the absence of polarons that are not stabilized on the phenazine segments of polyphenosafranine. The potential dependence of the ESR intensity of copolymer 3, with the



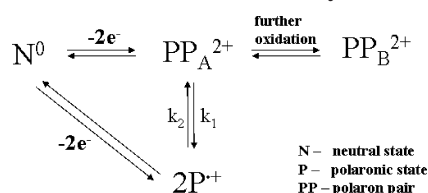


**Figure 15.** Potential dependence of current, ESR intensity, and absorbance at ca. 460 nm of (a) PANI and (b) copolymer 2, normalized to the maximum of the ESR intensity, and potential dependence of absorbance at different wavelengths of (c, e) PANI and (d, f) copolymer 2 during the forward scan in aqueous solution of 0.1 M sulfuric acid and 0.01 M sodium *p*-toluenesulfonate.

highest content of phenosafranine, differs from that of PANI for equal charges injected into the polymer layer (Figure 10c). In the case of the copolymer, an additional shoulder at 0.2 V is observed. This result will be discussed for the different chemical structures of PANI and copolymer and for the influence of the phenazine units in the polymer chain on polaron formation.

Therefore, polaron formation in PANI and its copolymers is stabilized on the linear segments of the polymer chains as is shown in Figure 11.

The UV/vis–NIR spectra of PANI and the copolymers during voltammetric scanning including the near-infrared region show a lot of absorption bands (Figure 12). Their potential dependence

**SCHEME 1: Scheme for Formation of Charged States upon Electrochemical Oxidation of Polyaniline**


is analyzed for both PANI and copolymer structures. The absorption peak at 310 nm decreases with increasing electrode potential and corresponds to the polymer segments in the reduced state. The absorbance at this wavelength is attributed to the  $\pi-\pi^*$  transition of benzenoid rings on the polymer chains. The UV/vis–NIR spectrum of the initial copolymer has an additional absorption peak at ca. 550 nm due to the presence of phenosafranine units in the polymer structure. The phenosafranine molecule has an absorption band at 520 nm, while the chemically and electrochemically prepared polyphenosafranine give the same peak at 530 and 550 nm, respectively (Figure 13a). The band at 550 nm in the absorption spectrum increases by anodic oxidation of the copolymer (Figure 13b). It corresponds to formation of conjugated 3,7-diamino-5-phenylphenazine, starting with the protonated nonconjugated 3,7-diamino-10-hydro-5-phenylphenazine rings.<sup>29</sup> The absorption peaks of the oxidized polymers at 290, 630, 1310, and 1420 nm are predominant at higher potentials, larger than the middle peak in the cyclovoltammogram. These peaks have their absorption maxima at +0.5 V. The band at 630 nm in reduced copolymer films is not observed because of the strong absorption peak at 550 nm. The peak at 620 nm was earlier attributed to the  $\pi-\pi^*$  transition of the nitrogen–quinone groups in polymer.<sup>42–45</sup> Masters et al.<sup>42</sup> attributed the peak at 283 nm to the quinoid structure of the pernigraniline base. The bands at 630, 1310, and 1420 nm are observed in the completely reduced state of polymer (Figure 14), because in the leucoemeraldine form of PANI there is a small percentage (3–4%) of quinoidic rings.<sup>46</sup> The four observed absorption bands at high electrode potential can be associated with the formation of quinoidic rings in polymer chains. The absorption peak at ca. 460 nm in both PANI and the copolymers under study increases with the charge injection before the ESR signal (Figure 15a,b). The potential dependence of the absorbance at 1280 and 1340 nm presents the same potential dependence as the peak at 460 nm (Figure 15c,d). These bands can be attributed to the formation of a spinless polaron pair (named *polaron pair A*).<sup>10</sup> The absorption bands at 1280 and 1340 nm are due to a splitting of the band structure in the valence band and the lowest level in the polaron pair. The potential dependence of the absorption bands at ca. 1100 and 1600 nm is the same as at 460 nm at low potentials (Figure 15e,f). These bands have their maxima at +0.25 V and decrease in the potential of the second anodic peak. Because the potential dependence of both these absorption bands differs from the potential dependence of polaron pair A, we propose the existence of a second polaron pair (named *polaron pair B*). Genies et al.<sup>20</sup> observed the same potential dependence of the absorption band of PANI at 831 nm as for the bands at 1100 and 1600 nm, which was attributed to an electron promotion from the valence band to a bonding level of the polaron–bipolaron. The absorption peak of the formed bipolaron, which gives only one absorption band from a dipole-allowed transition in the spectrum, might be hidden by the absorption of the polaron pairs.

Figure 15a,b demonstrates polaron formation in PANI and copolymer 2. The maximum of the ESR intensity in PANI and

the copolymer is observed at potentials higher than the first redox peak in the cyclovoltammogram. The potential difference between the half-peak current and the ESR intensity is 70–80 mV. Therefore, the formation of the polaron is delayed and at first the polaron pair is formed by two electron transfer products, which can dissociate into two polarons at higher potentials. The absorption peak of the polaron might be hidden by the absorption of the polaron pairs, but the existence of the polaron can be clearly proved by the simultaneous ESR measurements. Due to the shift of the maximum of polaron formation from the peak current, it can be concluded the polaron can be formed both by oxidation of the neutral polymer at higher potentials and by dissociation of the polaron pair at the lower potential range. A proposed mechanism for the formation of charged states in PANI upon oxidation is given in Scheme 1. At the early steps of charge injection, polaron pair A is formed. This polaron pair can dissociate into two polarons. Further oxidation of the polymer results at first in formation of the polaron and later in formation of polaron pair B. In general, in PANI the polaron can be formed both by oxidation of the neutral polymer and by dissociation of polaron pair A.

**Conclusions**

The formation of charged states in PANI containing phenazine-like structures was followed in detail by in situ ESR–UV/vis–NIR spectroelectrochemistry. At first it was demonstrated that copolymerization of aniline and phenosafranine is possible by electrochemical oxidation under potentiodynamic cycling. By comparison of the mass spectrometric analysis of polyaniline and the aniline–phenosafranine copolymers, the existence of phenazine-like structures in the polymer chains is proved. It was shown that the middle peak in the cyclovoltammogram of polyaniline is not associated with the presence of phenazine rings in polymer but with the presence of the benzoquinone/hydroquinone couple in the polymer structure. By use of the ESR measurements, it was shown that polarons are not stabilized on the phenazine segments of polymer film. Polaron formation in PANI and its copolymers is stabilized on the linear segments of the polymer chains. In situ ESR–UV/vis–NIR spectroelectrochemistry clearly demonstrated that polaron formation in polyaniline and copolymer occurs at higher electrode potentials than the charge into the polymer film. At the early stage of charge injection into the polymer, a *polaron pair* is formed as concluded from the absorption pattern. Further oxidation of the polymer results in formation first of the polaron and then of a *second polaron pair*. This stage of stabilization of the charge in polyaniline is different from the behavior of other conducting polymers. Finally, a mechanism of the formation of charged species in PANI is given, based on data from the in situ ESR–UV/vis–NIR spectroelectrochemical study.

**Acknowledgment.** We thank Dr. A. Petr, Dr. S. Klod, F. Ziegs, C. Malbrich, and M. Senf (all from IFW Dresden, Germany) for technical help and the Federal Ministry of Education and Research of Germany (BMBF) for financial support.

**References and Notes**

- (1) Heeger, A. J. *J. Phys. Chem. B* **2001**, *105*, 8475.
- (2) Novák, P.; Müller, K.; Santhanam, K. S. V.; Haas, O. *Chem. Rev.* **1997**, *97*, 207.
- (3) Argun, A. A.; Aubert, P.-H.; Thompson, B. C.; Schwendeman, I.; Gaupp, C. L.; Hwang, J.; Pinto, N. J.; Tanner, D. B.; MacDiarmid, A. G.; Reynolds, J. R. *Chem. Mater.* **2004**, *16*, 4401.

- (4) Lange, U.; Roznyatovskaya, N. V.; Mirsky, V. M. *Anal. Chim. Acta* **2008**, *614*, 1.
- (5) Saxena, V.; Malhotra, B. D. *Curr. Appl. Phys.* **2003**, *3*, 293.
- (6) Brédas, J. L.; Scott, J. C.; Yakushi, K.; Street, G. B. *Phys. Rev. B* **1984**, *30*, 1023.
- (7) Fesser, K.; Bishop, A. R.; Campbell, D. K. *Phys. Rev. B* **1983**, *27*, 4804.
- (8) Xia, Y.; Wiesinger, J. M.; MacDiarmid, A. G.; Epstein, A. *Chem. Mater.* **1995**, *7*, 443.
- (9) (a) Nicolau, Y. F.; Beadle, P. M.; Banka, E. *Synth. Met.* **1997**, *84*, 585. (b) Cochet, M.; Corraze, B.; Quillard, S.; Buisson, J. P.; Lefrant, S.; Louarn, G. *Synth. Met.* **1997**, *84*, 757.
- (10) Van Haare, J. A. E. H.; Havinga, E. E.; Van Dongen, J. L. J.; Janssen, R. A. J.; Cornil, J.; Brédas, J. L. *Chem.—Eur. J.* **1998**, *4*, 1509.
- (11) MacDiarmid, A. G.; Chiang, J. C.; Richter, A. F.; Epstein, A. J. *Synth. Met.* **1987**, *18*, 285.
- (12) Brazovskii, S.; Kirova, N.; Yu, Z. G.; Bishop, A. R.; Saxena, A. *Opt. Mater.* **1998**, *9*, 502.
- (13) Paasch, G.; Scheinert, S.; Petr, A.; Dunsch, L.; Russ, J. *Electrochemistry* **2006**, *42*, 1161.
- (14) (a) Hill, M. G.; Mann, K. R.; Miller, L. L.; Penneau, J. F. *J. Am. Chem. Soc.* **1992**, *114*, 2728. (b) Miller, L. L.; Mann, K. R. *Acc. Chem. Res.* **1996**, *29*, 417.
- (15) Petr, A.; Wei, D.; Kvarnström, C.; Ivaska, A.; Dunsch, L. *J. Phys. Chem. B* **2007**, *111*, 12395.
- (16) Smie, A.; Heinze, J. *Angew. Chem.* **1997**, *109*, 375.
- (17) Neudeck, A.; Petr, A.; Dunsch, L. *Synth. Met.* **1999**, *107*, 143.
- (18) Petr, A.; Dunsch, L. *J. Electroanal. Chem.* **1996**, *419*, 55.
- (19) Huang, W.-S.; Humphrey, B. D.; MacDiarmid, A. G. *J. Chem. Soc., Faraday Trans.* **1986**, *1*, 2385.
- (20) Genies, E. M.; Lapkowski, M.; Penneau, J. F. *J. Electroanal. Chem.* **1988**, *249*, 97.
- (21) Stilwell, D. E.; Park, S.-M. *J. Electrochem. Soc.* **1988**, *135*, 2254.
- (22) Harima, Y.; Jiang, X.; Patil, R.; Komaguchi, K.; Mizota, H. *Electrochim. Acta* **2007**, *52*, 8088.
- (23) Harima, Y.; Ogawa, F.; Patil, R.; Jiang, X. *Electrochim. Acta* **2007**, *52*, 3615.
- (24) Willstätter, R.; Moore, C. W. *Ber. Dtsch. Chem. Ges.* **1907**, *40*, 2665.
- (25) Green, A. G.; Woodhead, A. E. *Ber. Dtsch. Chem. Ges.* **1913**, *46*, 33.
- (26) Dunsch, L. Dissertation, Bergakademie Freiberg, Germany, 1973.
- (27) (a) Ćirić-Marjanović, G.; Trchová, M.; Stejskal, J. *J. Raman Spectrosc.* **2008**, *39*, 1375. (b) Trchová, M.; Šeděnková, I.; Konyushenko, E. N.; Stejskal, J.; Holler, P.; Ćirić-Marjanović, G. *J. Phys. Chem. B* **2006**, *110*, 9461. (c) Stejskal, J.; Sapurina, I.; Trchová, M.; Konyushenko, E. N.; Holler, P. *Polymer* **2006**, *47*, 8253.
- (28) (a) Do Nascimento, G. M.; Silva, C. H. B.; Izumi, C. M. S.; Temperini, M. L. A. *Spectrochim. Acta, Part A* **2008**, *71*, 869. (b) Do Nascimento, G. M.; Silva, C. H. B.; Temperini, M. L. A. *Polym. Degrad. Stab.* **2008**, *93*, 291. (c) Do Nascimento, G. M.; Temperini, M. L. A. *J. Raman Spectrosc.* **2008**, *39*, 772.
- (29) Komura, T.; Ishihara, M.; Yamaguchi, T.; Takahashi, K. *J. Electroanal. Chem.* **2000**, *493*, 84.
- (30) Ćirić-Marjanović, G.; Blinova, N. V.; Trchová, M.; Stejskal, J.; Holler, P. *J. Phys. Chem. B* **2007**, *111*, 2188.
- (31) Rapta, P.; Neudeck, A.; Petr, A.; Dunsch, L. *J. Chem. Soc., Faraday Trans.* **1998**, *94*, 3625.
- (32) Dunsch, L. *J. Prakt. Chem.* **1975**, *317*, 409.
- (33) Stammer, C.; Taurins, A. *Spectrochim. Acta* **1963**, *19*, 1625.
- (34) Mitchell, M. B.; Smith, G. R.; Guillory, W. A. *J. Chem. Phys.* **1981**, *75*, 44.
- (35) Pouchert, C. J. *The Aldrich Library of FT-IR Spectra*, 2nd ed.; Aldrich Chemical Co.: Milwaukee, WI, 1985.
- (36) Chiba, K.; Ohsaka, T.; Ohnuki, Y.; Oyama, N. *J. Electroanal. Chem.* **1987**, *219*, 117.
- (37) Socrates, G. *Infrared and Raman characteristic group frequencies*; Wiley: New York, 2001.
- (38) Chiang, J.-C.; MacDiarmid, A. G. *Synth. Met.* **1986**, *13*, 193.
- (39) Šeděnková, I.; Trchová, M.; Stejskal, J. *Polym. Degrad. Stab.* **2008**, *93*, 2147.
- (40) Tang, J.; Jing, X.; Wang, B.; Wang, F. *Synth. Met.* **1988**, *24*, 231.
- (41) Surwade, S. P.; Dua, V.; Manohar, N.; Manohar, S. K.; Beck, E.; Ferraris, J. P. *Synth. Met.* **2009**, *159*, 445.
- (42) Masters, J. G.; Sun, Y.; MacDiarmid, A. G.; Epstein, A. J. *Synth. Met.* **1991**, *41*, 715.
- (43) Inoue, M.; Navarro, R. E.; Inoue, M. B. *Synth. Met.* **1989**, *30*, 199.
- (44) Duke, C. B.; Conwell, E. M.; Paton, A. *Chem. Phys. Lett.* **1986**, *131*, 82.
- (45) Stafström, S.; Bredas, J. L.; Epstein, A. J.; Woo, H. S.; Tanner, D. B.; Huang, W. S.; MacDiarmid, A. G. *Phys. Rev. Lett.* **1987**, *59*, 1464.
- (46) McCall, R. P.; Ginder, J. M.; Leng, J. M.; Ye, H. J.; Manohar, S. K.; Masters, J. G.; Asturias, G. E.; MacDiarmid, A. G.; Epstein, A. J. *Phys. Rev. B* **1990**, *41*, 5202.